A Simple Sliding Mode Controller of a Fifth-Order Nonlinear PEM Fuel Cell Model

Gunhyung Park, *Student Member, IEEE*, and Zoran Gajic, *Senior Member, IEEE*

***Abstract*—This paper presents a nonlinear control strategy for the well-known nonlinear fifth-order model of a proton exchange membrane (PEM, also known as polymer electrolyte membrane) fuel cell (PEMFC). We propose a simple sliding mode technique for this nonlinear model to keep pressures of hydrogen and oxygen at the desired values despite of changes of the fuel cell current. It is known that large deviations between hydrogen and oxygen partial pressures can damage the fuel cell membrane. The controller keeps the pressure difference between hydrogen and oxygen as small as possible after reaching steady state. Since the fuel cell current is considered as a disturbance, we apply a sliding mode control technique that copes well with external disturbances and uncertainties. Moreover, the proposed controller outperforms the controller previously proposed for this fuel cell model.**

***Index Terms*—Nonlinear control, PEM fuel cell, sliding mode control.**

I. Introduction

FUEL cells are electrochemical energy devices that convert chemical energy into electricity, heat, and water without generating carbon dioxide. Fuel cells are one of the most promising clean energy technologies among renewable energy sources since they have high efficiency and low environmental pollution. Among various fuel cells, proton exchange membrane fuel cells (PEMFCs) are the most developed and popular type of fuel cells. They use hydrogen as the fuel and have good features such as solid electrolyte (which reduces corrosion and electrolyte management problems), low temperature, and quick start-up. The schematic of PEMFCs is shown in Fig. 1. The hydrogen fed to the anode side produces H^+ ions (protons) and electrons with a help of a catalyst. Since the membrane allows only H^+ ions to pass through, the electrons reach the cathode side through an outside electrical circuit. In the cathode side, the diffusing H^+ and electrons combine with the supplied oxygen and form water. Applications of fuel cells include automobile, mobile devices, residential power generation, and backup generators. From the system theory point of view, PEMFCs represent nonlinear, multiple-input multiple-output dynamic systems [1].

From the modeling and control view point, several models have been proposed. Third-order linear model of PEMFC was developed in [2] and a third-order bilinear model of PEMFC was derived in [3]. Chiu *et al.* [4] considered the third-order nonlinear model, and Na and Gou established a fifth-order nonlinear model in [5]. Chiu and his coworkers [4] indicated a need for using a higher order dimensional model that includes dynamics of anode water needed for membrane humidification and cathode nitrogen (that comes from pumped air), see Fig. 2. A nonlinear ninth-order model of PEMFC was derived in [6] and its simplified fourth- and sixth-order variants were presented in [7] and [8].

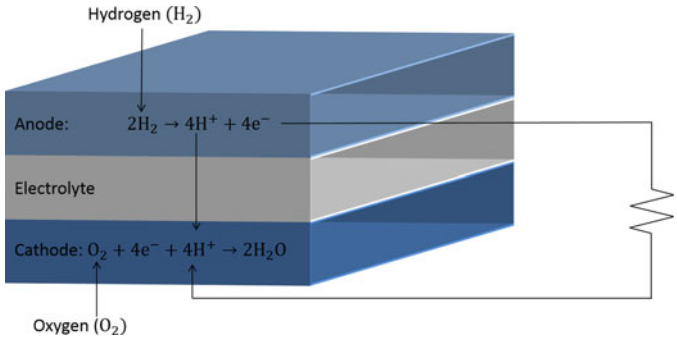

Fig. 1. Schematic of PEMFCs.

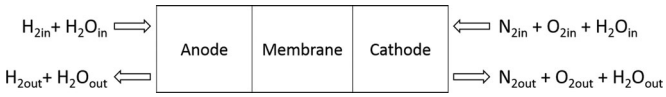

Fig. 2. Gas flows of PEMFC's model in [5].

In the last few years, several control strategies for PEMFC are proposed including a sliding mode control technique that is robust against disturbances [7]–[13]. A sliding mode controller is designed for the model of [7] using for the sliding variable the difference between the actual and nominal angular air compressor speeds. Kunusch and his coworkers [8] have considered a second-order sliding mode controller for the breathing subsystem of a PEMFC stack focusing on the chattering phenomenon based on the model of Pukrushpan *et al.* [6]. In [9], a second-order sliding mode controller ("twisting algorithm") is also used for the nonlinear model developed by the authors utilizing the results of [6] and [7]. In [10], an oxygen flow problem with real-time implementation of a sliding mode controller has been considered. The hybrid controller composed of an internal mode control based PID (proportional-integral-derivative) control and an adaptive sliding mode controller has been designed in [11]. The first controller is used for the hydrogen reformer and the second controller is used for the PEMFC model based on the

Manuscript received December 17, 2012; revised September 27, 2013; accepted October 21, 2013. Date of publication November 12, 2013; date of current version February 14, 2014. Paper no. TEC-00671-2012.

The authors are with the Department of Electrical and Computer Engineering, Rutgers University, Piscataway, NJ 08854 USA (e-mail: gunhyung@ece.rutgers.edu; gajic@ece.rutgers.edu).

Color versions of one or more of the figures in this paper are available online at http://ieeexplore.ieee.org.

Digital Object Identifier 10.1109/TEC.2013.2288064

work of El-Sharkh *et al.* [2]. In [12], a rapid-convergent sliding mode controller for the temperature control system of PEMFC stack has been presented. The sliding mode control design for the *linearized* model of [5] was presented in [13]. Sliding mode control designs for the fuel cell connection to an electric grid have been presented in [14]–[17].

In this paper, we propose a nonlinear sliding mode controller design for the fifth-order nonlinear model of PEMFC developed in [5], see also the recent book [18]. The purpose of the controller proposed in this paper is to keep small the difference of hydrogen and oxygen pressures to prevent the membrane damage. Since there exist uncertainties ($p_{\mathrm{H_2O_A}}(t)$, $p_{\mathrm{O_2}}(t)$, and $p_{\mathrm{H_2O_C}}(t)$) and a disturbance ($I(t)$), a sliding mode controller, which is robust against disturbances and uncertainties, is proposed. It will be seen from the simulation results that the sliding mode controller proposed in this paper outperforms the feedback linearization-based controller proposed in [5].

The state space model of [5] is given as follows:

$$\begin{aligned}
\dot{x}_1(t) &= \frac{RT\lambda_{\mathrm{H_2}}}{V_{\mathrm{A}}}\left(\Upsilon_{\mathrm{H_2}} - \frac{x_1(t)}{x_1(t)+x_2(t)}\right)k_{\mathrm{a}}u_{\mathrm{a}}(t) \\
&\quad + \frac{RTC_1(1-\gamma)}{V_{\mathrm{A}}}\left(\frac{x_1(t)}{x_1(t)+x_2(t)} - 1\right)I(t) \\
\dot{x}_2(t) &= \frac{RT\lambda_{\mathrm{H_2}}}{V_{\mathrm{A}}}\left(\frac{\varphi_{\mathrm{a}}P_{\mathrm{vs}}}{x_1(t)+x_2(t)-\varphi_{\mathrm{a}}P_{\mathrm{vs}}} - \frac{x_2(t)}{x_1(t)+x_2(t)}\right) \\
&\quad \times k_{\mathrm{a}}u_{\mathrm{a}}(t) + \frac{RTC_1}{V_{\mathrm{A}}}\left(\frac{x_2(t)}{x_1(t)+x_2(t)} - 1\right)I(t) \\
\dot{x}_3(t) &= \frac{RT\lambda_{\mathrm{air}}}{V_{\mathrm{C}}}\left(\Upsilon_{\mathrm{O_2}} - \frac{x_3(t)}{x_3(t)+x_4(t)+x_5(t)}\right)k_{\mathrm{c}}u_{\mathrm{c}}(t) \\
&\quad + \frac{RTC_1}{2V_{\mathrm{C}}}\left(\frac{x_3(t)}{x_3(t)+x_4(t)+x_5(t)} - 1\right)I(t) \\
\dot{x}_4(t) &= \frac{RT\lambda_{\mathrm{air}}}{V_{\mathrm{C}}}\left(\Upsilon_{\mathrm{N_2}} - \frac{x_4(t)}{x_3(t)+x_4(t)+x_5(t)}\right)k_{\mathrm{c}}u_{\mathrm{c}}(t) \\
\dot{x}_5(t) &= \frac{RT\lambda_{\mathrm{air}}}{V_{\mathrm{C}}}\left(\frac{\varphi_{\mathrm{a}}P_{\mathrm{vs}}}{x_3(t)+x_4(t)+x_5(t)-\varphi_{\mathrm{a}}P_{\mathrm{vs}}}\right. \\
&\quad \left. - \frac{x_5(t)}{x_3(t)+x_4(t)+x_5(t)}\right)k_{\mathrm{c}}u_{\mathrm{c}}(t) \\
&\quad + \frac{RTC_1(1-\gamma)}{V_{\mathrm{C}}}\left(\frac{C_2}{C_1}\left(1 - \frac{x_5(t)}{x_3(t)+x_4(t)+x_5(t)}\right)\right. \\
&\quad \left. - 1 - \frac{x_5(t)}{x_3(t)+x_4(t)+x_5(t)}\right)I(t). \qquad (1)
\end{aligned}$$

The state variables in this model represent respectively pressures of hydrogen and water at the anode side and pressures of oxygen, nitrogen, and water at the cathode side, that is

$$\begin{aligned}
x(t) &= [\, x_1(t) \quad x_2(t) \quad x_3(t) \quad x_4(t) \quad x_5(t)\,]^T \\
&= [\, p_{\mathrm{H_2}}(t) \quad p_{\mathrm{H_2O_A}}(t) \quad p_{\mathrm{O_2}}(t) \quad p_{\mathrm{N_2}}(t) \quad p_{\mathrm{H_2O_C}}(t)\,]^T. \qquad (2)
\end{aligned}$$

The model output variables are

$$y(t) = \begin{bmatrix} x_1(t) \\ x_3(t) \end{bmatrix} = \begin{bmatrix} p_{\mathrm{H_2}}(t) \\ p_{\mathrm{O_2}}(t) \end{bmatrix}. \qquad (3)$$

TABLE I
PARAMETERS OF THE FUEL CELL

Symbol	Parameter	Value [Unit]
R	Gas constant	8.314 [J mol^{-1} K^{-1}]
T	Operating cell temperature	353 [K]
N	Number of cells	35
V_{A}	Anode volume	0.005 [m^3]
V_{C}	Cathode volume	0.010 [m^3]
k_{a}	Anode conversion factor	7.034×10^{-4} [mol s^{-1}]
k_{c}	Cathode conversion factor	7.036×10^{-4} [mol s^{-1}]
A	Fuel cell active area	232×10^{-4} [m^2]
F	Faraday constant	96,485 [A s mol^{-1}]
P_{vs}	Saturation pressure	32 [kPa]
$\Upsilon_{\mathrm{O_2}}$	O_2 reactant fraction	0.2095
$\Upsilon_{\mathrm{N_2}}$	N_2 reactant fraction	0.7808
$\Upsilon_{\mathrm{H_2}}$	H_2 reactant fraction	0.9999
C_1	$N \cdot A/2F$	4.21×10^{-6} [m^2 mol A^{-1} s^{-1}]
C_2	$1.2684N \cdot A/F$	1.07×10^{-5} [m^2 mol A^{-1} s^{-1}]
$\lambda_{\mathrm{H_2}}$	H_2 stoichiometric constant	2
λ_{air}	Air stoichiometric constant	2.5
φ_{a}	Anode humidity constant	0.8
φ_{c}	Cathode humidity constant	0.9

In model (1), R is the universal gas constant, T is temperature, and V_{A}, V_{C} are anode and cathode volumes, C_1, C_2 are known constants [5], [18], φ_{a}, φ_{c} are the relative humidity constants, P_{vs} is the saturation pressure, $\lambda_{\mathrm{H_2}}$, λ_{air} are stoichiometric constants, and $\Upsilon_{\mathrm{H_2}} = 0.99$, $\Upsilon_{\mathrm{O_2}} = 0.21$, $\Upsilon_{\mathrm{N_2}} = 0.79$ are reactant fractions [5], [13], [18]. $I(t)$ is the cell current, and it is considered as a disturbance since it changes as $V_{\mathrm{fc}}/R_{\mathrm{L}}$, where V_{fc} is the produced fuel cell voltage and R_{L} is the load of active users (sum of their resistances), which changes randomly. γ is the coefficient measured experimentally in [19] for the back-diffusion of water from the cathode to the anode sides, which is defined as $H_2O_{\mathrm{back}} = \gamma H_2O_{\mathrm{mbr}}$ where H_2O_{back} is the water back-diffusion flow rate and H_2O_{mbr} is the membrane water inlet flow rate [18]. In this model, it is assumed that the water in the system is perfectly controlled and the back-diffusion is not considered, which means γ is zero. The numeric values of the defined quantities are presented in Table I. It should be pointed out that the outlet $p_{\mathrm{H_2}}(t)$ and $p_{\mathrm{O_2}}(t)$ are typically lower than the gas pressure in contact with membrane.

The system control input is $u(t) = [\, u_{\mathrm{a}}(t) \quad u_{\mathrm{c}}(t)\,]^T$,

$$u_{\mathrm{a}}(t) = \frac{1}{k_{\mathrm{a}}}\big(H_{2\mathrm{in}}(t) + H_2O_{\mathrm{Ain}}(t)\big) \qquad (4)$$

$$u_{\mathrm{c}}(t) = \frac{1}{k_{\mathrm{c}}}\big(O_{2\mathrm{in}}(t) + N_{2\mathrm{in}}(t) + H_2O_{\mathrm{Cin}}(t)\big) \qquad (5)$$

$H_{2\mathrm{in}}(t)$, $H_2O_{\mathrm{Ain}}(t)$, $O_{2\mathrm{in}}(t)$, $N_{2\mathrm{in}}(t)$, and $H_2O_{\mathrm{Cin}}(t)$ represent inlet flow rates of hydrogen, water vapor at the anode side, oxygen, nitrogen, and water vapor at the cathode side, respectively, k_{a} and k_{c} are known constants.

II. SLIDING MODE CONTROL FOR THE FIFTH-ORDER PEMFC MODEL

Sliding mode control is a form of variable structure control [20], where sliding surfaces are designed such that systems trajectories exhibit desirable properties. A system using sliding mode control has been considered as a robust system, which yields to the reduced system sensitivity to uncertainties

and exogenous disturbances. Sliding mode control systems have been studied in different setups by many researchers [20]. The controller is designed in two steps—finding the sliding surface and reaching the sliding mode. First, a sliding surface is defined which ensures that the system remains on a hyperplane after reaching it from any initial condition in a finite time. Second, discontinuous control is designed to render a sliding mode. Approaches [20]–[23] can be used for linear continuous-time sliding mode control, which has been recognized as a robust control approach, that yields rejection of matched disturbances and system uncertainties.

In the following, we present the sliding mode control technique for the fifth-order nonlinear PEMFC model (1)–(3). Our goal is to design a sliding mode surface and find a control law such that the output $y(t)$ tracks a constant reference y_{desired}. The sliding manifold is defined as follows (since the relative degree of the system is one for both inputs [24]):

$$s(t) = \begin{bmatrix} s_1(t) \\ s_2(t) \end{bmatrix} = e(t) = \begin{bmatrix} e_1(t) \\ e_2(t) \end{bmatrix} = y(t) - y_{\text{desired}} = 0 \tag{6}$$

$e_{\text{i}}(t)$ is the error between the output $y_{\text{i}}(t)$ and $y_{\text{i}_{\text{desired}}}$. Specifically, $s(t) = 0$ implies that the pressure error is zero. It can be shown that expressions for the control inputs appear in the equation for $\dot{s}(t)$, that is

$$\begin{aligned} \dot{s}(t) &= \begin{bmatrix} \dot{s}_1(t) \\ \dot{s}_2(t) \end{bmatrix} = \dot{y}(t) = \begin{bmatrix} \dot{x}_1(t) \\ \dot{x}_3(t) \end{bmatrix} \\ &= \begin{bmatrix} \frac{RT\lambda_{\text{H}_2}}{V_{\text{A}}}\left(\Upsilon_{\text{H}_2} - \frac{x_1(t)}{x_1(t)+x_2(t)}\right)k_{\text{a}}u_{\text{a}}(t) \\ \quad + \frac{RTC_1}{V_{\text{A}}}\left(\frac{x_1(t)}{x_1(t)+x_2(t)} - 1\right)I(t) \\ \frac{RT\lambda_{\text{air}}}{V_{\text{C}}}\left(\Upsilon_{\text{O}_2} - \frac{x_3(t)}{x_3(t)+x_4(t)+x_5(t)}\right)k_{\text{c}}u_{\text{c}}(t) \\ \quad + \frac{RTC_1}{2V_{\text{C}}}\left(\frac{x_3(t)}{x_3(t)+x_4(t)+x_5(t)} - 1\right)I(t) \end{bmatrix}. \end{aligned} \tag{7}$$

Note that

$$\begin{aligned} \Upsilon_{\text{H}_2} - \frac{x_1(t)}{x_1(t)+x_2(t)} > 0 \\ \Upsilon_{\text{O}_2} - \frac{x_3(t)}{x_3(t)+x_4(t)+x_5(t)} > 0 \end{aligned} \tag{8}$$

since

$$\begin{aligned} \Upsilon_{\text{H}_2} = 0.99 \simeq 1 \geq \frac{p_{\text{H}_2}}{p_{\text{H}_2} + p_{H_2O_A}} \\ \Upsilon_{\text{O}_2} = 0.79 = \frac{p_{\text{O}_2}}{p_{\text{O}_2} + p_{\text{N}_2}} \geq \frac{p_{\text{O}_2}}{p_{\text{O}_2} + p_{\text{N}_2} + p_{H_2O_C}}. \end{aligned} \tag{9}$$

We assume that the current changes are bounded as

$$0 < I_{\min} < I(t) < I_{\max}. \tag{10}$$

The sliding mode control laws have to satisfy the following sliding mode condition [20]:

$$s_i(t)\dot{s}_i(t) < 0,\ i = 1, 2. \tag{11}$$

From (7)–(10), we have

$$\begin{aligned} &\dot{s}_1(t) \\ &= \begin{cases} \frac{RTC_1}{V_{\text{A}}}\left(1 - \frac{x_1(t)}{x_1(t)+x_2(t)}\right)\left(I_{\min} - I(t)\right) \\ \quad - \frac{RT\lambda_{\text{H}_2}}{V_{\text{A}}}\left(\Upsilon_{\text{H}_2} - \frac{x_1(t)}{x_1(t)+x_2(t)}\right)k_{\text{a}}\sigma_1\text{sat}\left(s_1(t)\right) < 0 \\ \qquad\qquad \text{if } s_1(t) > 0 \\ \frac{RTC_1}{V_{\text{A}}}\left(1 - \frac{x_1(t)}{x_1(t)+x_2(t)}\right)\left(I_{\max} - I(t)\right) \\ \quad - \frac{RT\lambda_{\text{H}_2}}{V_{\text{A}}}\left(\Upsilon_{\text{H}_2} - \frac{x_1(t)}{x_1(t)+x_2(t)}\right)k_{\text{a}}\sigma_2\text{sat}\left(s_1(t)\right) > 0 \\ \qquad\qquad \text{if } s_1(t) < 0 \end{cases} \\ &\dot{s}_2(t) \\ &= \begin{cases} \frac{RTC_1}{2V_{\text{C}}}\left(1 - \frac{x_3(t)}{x_3(t)+x_4(t)+x_5(t)}\right)\left(I_{\min} - I(t)\right) \\ \quad - \frac{RT\lambda_{\text{air}}}{V_{\text{C}}}\left(\Upsilon_{\text{O}_2} - \frac{x_3(t)}{x_3(t)+x_4(t)+x_5(t)}\right)k_{\text{c}}\sigma_3\text{sat}\left(s_2(t)\right) < 0 \\ \qquad\qquad \text{if } s_2(t) > 0 \\ \frac{RTC_1}{2V_{\text{C}}}\left(1 - \frac{x_3(t)}{x_3(t)+x_4(t)+x_5(t)}\right)\left(I_{\max} - I(t)\right) \\ \quad - \frac{RT\lambda_{\text{air}}}{V_{\text{C}}}\left(\Upsilon_{\text{O}_2} - \frac{x_3(t)}{x_3(t)+x_4(t)+x_5(t)}\right)k_{\text{c}}\sigma_4\text{sat}\left(s_2(t)\right) > 0 \\ \qquad\qquad \text{if } s_2(t) < 0 \end{cases} \end{aligned} \tag{12}$$

since

$$\begin{aligned} &\frac{RTC_1}{V_{\text{A}}}\left(\frac{x_1(t)}{x_1(t)+x_2(t)} - 1\right)I = -\frac{RTC_1}{V_{\text{A}}}\frac{x_2(t)}{x_1(t)+x_2(t)}I < 0 \\ &\frac{RTC_1}{2V_{\text{C}}}\left(\frac{x_3(t)}{x_3(t)+x_4(t)+x_5(t)} - 1\right)I \\ &\qquad = -\frac{RTC_1}{2V_{\text{C}}}\frac{x_4(t)+x_5(t)}{x_3(t)+x_4(t)+x_5(t)}I < 0. \end{aligned} \tag{13}$$

Note that $I(t) - I_{\min} > 0$ and $I_{\max} - I(t) > 0$.

We can design the control laws, satisfying (11), as follows [following the unit sliding mode control design of [20] taking into account constraint (10)]:

$$u_{\text{a}}(t) = \begin{cases} -\frac{C_1\left(\frac{x_1(t)}{x_1(t)+x_2(t)} - 1\right)I_{\min}}{\lambda_{\text{H}_2}\left(\Upsilon_{\text{H}_2} - \frac{x_1(t)}{x_1(t)+x_2(t)}\right)k_{\text{a}}} - \sigma_1\text{sat}\left(s_1(t)\right) \\ \qquad\qquad \text{if } s_1(t) > 0 \\ -\frac{C_1\left(\frac{x_1(t)}{x_1(t)+x_2(t)} - 1\right)I_{\max}}{\lambda_{\text{H}_2}\left(\Upsilon_{\text{H}_2} - \frac{x_1(t)}{x_1(t)+x_2(t)}\right)k_{\text{a}}} - \sigma_2\text{sat}\left(s_1(t)\right) \\ \qquad\qquad \text{if } s_1(t) < 0 \end{cases} \tag{14}$$

and

$$u_{\text{c}}(t) = \begin{cases} -\frac{C_1\left(\frac{x_3(t)}{x_3(t)+x_4(t)+x_5(t)} - 1\right)I_{\min}}{2\lambda_{\text{air}}\left(\Upsilon_{\text{O}_2} - \frac{x_3(t)}{x_3(t)+x_4(t)+x_5(t)}\right)k_{\text{c}}} - \sigma_3\text{sat}\left(s_2(t)\right) \\ \qquad\qquad \text{if } s_2(t) > 0 \\ -\frac{C_1\left(\frac{x_3(t)}{x_3(t)+x_4(t)+x_5(t)} - 1\right)}{2\lambda_{\text{air}}\left(\Upsilon_{\text{O}_2} - \frac{x_3(t)}{x_3(t)+x_4(t)+x_5(t)}\right)k_{\text{c}}} - \sigma_4\text{sat}\left(s_2(t)\right) \\ \qquad\qquad \text{if } s_2(t) < 0 \end{cases} \tag{15}$$

where $\sigma_i > 0,\ i = 1, 2, 3, 4$ are used for adjusting the speed of reaching the sliding surfaces. σ_1 and σ_3 should provide $u_{\rm a}(t) > 0$ and $u_{\rm c}(t) > 0$ since $u_{\rm a}(t)$ and $u_{\rm c}(t)$ are the flow rates. σ_2 and σ_4 should be chosen according to the upper limits of $u_{\rm a}(t)$ ($u_{\rm a_{max}}$) and $u_{\rm c}(t)$ ($u_{\rm c_{max}}$).

The controllers in (14)–(15) use the state variables which are not known except for $x_1(t)$ and $x_3(t)$. Instead of using a nonlinear observer to observe the states, we can design the controller assuming $K_1 \leqslant \frac{1-\frac{x_1(t)}{x_1(t)+x_2(t)}}{\Upsilon_{\rm H_2}-\frac{x_1(t)}{x_1(t)+x_2(t)}} \leqslant K_2$ and $K_3 \leqslant \frac{1-\frac{x_3(t)}{x_3(t)+x_4(t)+x_5(t)}}{\Upsilon_{\rm O_2}-\frac{x_3(t)}{x_3(t)+x_4(t)+x_5(t)}} \leqslant K_4$.

The simplified control laws can be found from (14) and (15) as follows:

$$u_{\rm a}(t) = \begin{cases} -\frac{K_1 C_1 I_{\min}}{\lambda_{\rm H_2} k_{\rm a}} - \sigma_1 {\rm sat}\big(s_1(t)\big) & \text{if } s_1(t) > 0 \\ -\frac{K_2 C_1 I_{\max}}{\lambda_{\rm H_2} k_{\rm a}} - \sigma_2 {\rm sat}\big(s_1(t)\big) & \text{if } s_1(t) < 0 \end{cases} \tag{16}$$

$$u_{\rm c}(t) = \begin{cases} -\frac{K_3 C_1 I_{\min}}{2\lambda_{\rm air} k_{\rm c}} - \sigma_3 {\rm sat}\big(s_2(t)\big) & \text{if } s_2(t) > 0 \\ -\frac{K_4 C_1 I_{\max}}{2\lambda_{\rm air} k_{\rm c}} - \sigma_4 {\rm sat}\big(s_2(t)\big) & \text{if } s_2(t) < 0. \end{cases} \tag{17}$$

These *simplified* control laws (16) and (17) will be also implemented in our simulation study.

Using formula (16), $\dot{s}_1(t)$ in (7) can be expressed as

$$\begin{aligned} \dot{s}_1(t) &= \frac{K_1 RTC_1}{V_{\rm A}}\left(\Upsilon_{\rm H_2} - \frac{x_1(t)}{x_1(t)+x_2(t)}\right) I_{\min} \\ &\quad + \frac{RTC_1}{V_{\rm A}}\left(\frac{x_1(t)}{x_1(t)+x_2(t)} - 1\right) I(t) \\ &\quad - \frac{RT\lambda_{\rm H_2}}{V_{\rm A}}\left(\Upsilon_{\rm H_2} - \frac{x_1(t)}{x_1(t)+x_2(t)}\right) k_{\rm a}\sigma_1 {\rm sat}\big(s_1(t)\big) \\ &= \frac{RTC_1}{V_{\rm A}}\left(\left(\Upsilon_{\rm H_2} - \frac{x_1(t)}{x_1(t)+x_2(t)}\right) K_1 I_{\min} \right. \\ &\quad \left. - \left(1 - \frac{x_1(t)}{x_1(t)+x_2(t)}\right) I(t)\right) \\ &\quad - \frac{RT\lambda_{\rm H_2}}{V_{\rm A}}\left(\Upsilon_{\rm H_2} - \frac{x_1(t)}{x_1(t)+x_2(t)}\right) k_{\rm a}\sigma_1 {\rm sat}\big(s_1(t)\big) < 0 \end{aligned} \tag{18}$$

when $s_1(t) > 0$, and

$$\begin{aligned} \dot{s}_1(t) &= \frac{K_2 RTC_1}{V_{\rm A}}\left(\Upsilon_{\rm H_2} - \frac{x_1(t)}{x_1(t)+x_2(t)}\right) I_{\max} \\ &\quad + \frac{RTC_1}{V_{\rm A}}\left(\frac{x_1(t)}{x_1(t)+x_2(t)} - 1\right) I(t) \\ &\quad - \frac{RT\lambda_{\rm H_2}}{V_{\rm A}}\left(\Upsilon_{\rm H_2} - \frac{x_1(t)}{x_1(t)+x_2(t)}\right) k_{\rm a}\sigma_2 {\rm sat}\big(s_1(t)\big) \\ &= \frac{RTC_1}{V_{\rm A}}\left(\left(\Upsilon_{\rm H_2} - \frac{x_1(t)}{x_1(t)+x_2(t)}\right) K_2 I_{\max} \right. \\ &\quad \left. - \left(1 - \frac{x_1(t)}{x_1(t)+x_2(t)}\right) I(t)\right) \\ &\quad - \frac{RT\lambda_{\rm H_2}}{V_{\rm A}}\left(\Upsilon_{\rm H_2} - \frac{x_1(t)}{x_1(t)+x_2(t)}\right) k_{\rm a}\sigma_2 {\rm sat}\big(s_1(t)\big) > 0 \end{aligned} \tag{19}$$

when $s_1(t) < 0$.

Similarly, condition (11) for $s_2(t)$ can be checked using (17) and (7). For $s_2(t) > 0$, we have

$$\begin{aligned} &\dot{s}_2(t) \\ &= \frac{K_3 RTC_1}{2V_{\rm C}}\left(\Upsilon_{\rm O_2} - \frac{x_3(t)}{x_3(t)+x_4(t)+x_5(t)}\right) I_{\min} \\ &\quad + \frac{RTC_1}{2V_{\rm C}}\left(\frac{x_3(t)}{x_3(t)+x_4(t)+x_5(t)} - 1\right) I(t) \\ &\quad - \frac{RT\lambda_{\rm air}}{V_{\rm C}}\left(\Upsilon_{\rm O_2} - \frac{x_3(t)}{x_3(t)+x_4(t)+x_5(t)}\right) k_{\rm c}\sigma_3 {\rm sat}\big(s_2(t)\big) \\ &= \frac{RTC_1}{2V_{\rm C}}\left(\left(\Upsilon_{\rm O_2} - \frac{x_3(t)}{x_3(t)+x_4(t)+x_5(t)}\right) K_3 I_{\min} \right. \\ &\quad \left. - \left(1 - \frac{x_3(t)}{x_3(t)+x_4(t)+x_5(t)}\right) I(t)\right) \\ &\quad - \frac{RT\lambda_{\rm air}}{V_{\rm C}}\left(\Upsilon_{\rm O_2} - \frac{x_3(t)}{x_3(t)+x_4(t)+x_5(t)}\right) k_{\rm c}\sigma_3 {\rm sat}\big(s_2(t)\big) \\ &\quad < 0 \end{aligned} \tag{20}$$

and for $s_2(t) < 0$, we obtain

$$\begin{aligned} &\dot{s}_2(t) \\ &= \frac{K_4 RTC_1}{2V_{\rm C}}\left(\Upsilon_{\rm O_2} - \frac{x_3(t)}{x_3(t)+x_4(t)+x_5(t)}\right) I_{\max} \\ &\quad + \frac{RTC_1}{2V_{\rm C}}\left(\frac{x_3(t)}{x_3(t)+x_4(t)+x_5(t)} - 1\right) I(t) \\ &\quad - \frac{RT\lambda_{\rm air}}{V_{\rm C}}\left(\Upsilon_{\rm O_2} - \frac{x_3(t)}{x_3(t)+x_4(t)+x_5(t)}\right) k_{\rm c}\sigma_4 {\rm sat}\big(s_2(t)\big) \\ &= \frac{RTC_1}{2V_{\rm C}}\left(\left(\Upsilon_{\rm O_2} - \frac{x_3(t)}{x_3(t)+x_4(t)+x_5(t)}\right) K_4 I_{\max} \right. \\ &\quad \left. - \left(1 - \frac{x_3(t)}{x_3(t)+x_4(t)+x_5(t)}\right) I(t)\right) \\ &\quad - \frac{RT\lambda_{\rm air}}{V_{\rm C}}\left(\Upsilon_{\rm O_2} - \frac{x_3(t)}{x_3(t)+x_4(t)+x_5(t)}\right) k_{\rm c}\sigma_4 {\rm sat}\big(s_2(t)\big) \\ &\quad > 0. \end{aligned} \tag{21}$$

K_1, K_2, K_3, and K_4 can be found explicitly from simulations using control laws of (14) and (15).

III. Simulation Example

The numerical data taken from [5], used in this paper, are presented in Table I. The objective is to keep the pressure differences between hydrogen and oxygen in a certain range to protect membrane damages when control inputs are limited to: 0 slpm[1]

[1]slpm stands for the standard liter per minute unit.

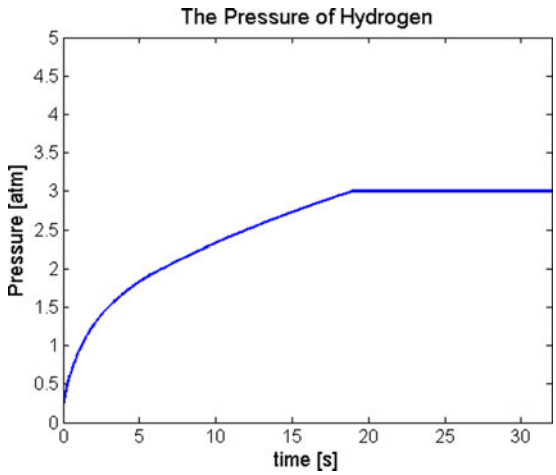

Fig. 3. Pressure of hydrogen for the nonlinear system under controller (14).

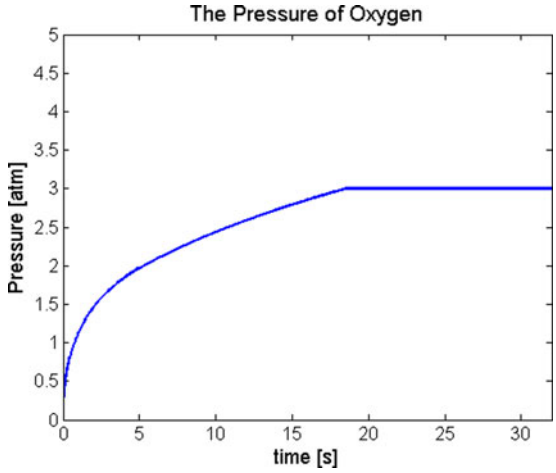

Fig. 4. Pressure of oxygen for the nonlinear system under controller (15).

$<$ input flow rate of hydrogen or oxygen ([slpm]) $<$ 10 slpm. We have designed the controller to keep both pressures around 3 atm. We have also required that the controller reduces the hydrogen and oxygen pressure differences during the transient state.

The simulation results for hydrogen and oxygen pressures are presented in Figs. 3 and 4 with the disturbance current waveform presented in Fig. 5. It can be noticed from Figs. 3 and 4 that the pressures are kept around 3 atm after reaching the desired steady-state values after about 19 s despite the abrupt current changes. The corresponding control laws are presented in Figs. 6 and 7. After entering the sliding mode at about 19 s, the flow rate changes are needed to make $s_i(t) = 0,\ i = 1, 2$, at some points as seen in the zoom-in of the plots in Figs. 6 and 7.

Since we only know $x_1(t)$ and $x_3(t)$ from the output equation, using the *simplified* controllers defined in (16) and (17), the pressures of hydrogen and oxygen can be also regulated. The corresponding simulation results obtained for $K_1 = 1.0003$, $K_2 = 1.2$, $K_3 = 1.3715$, and $K_4 = 1.3833$ are shown in Figs. 8–11. They indicate that the pressures and control signals have very similar trajectories of those of Figs. 3, 4, 6, and 7.

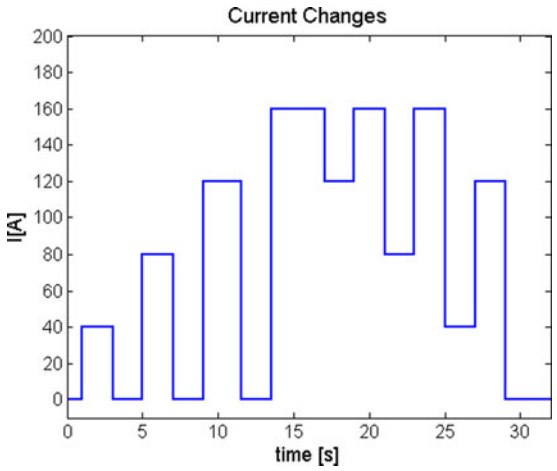

Fig. 5. Current changes.

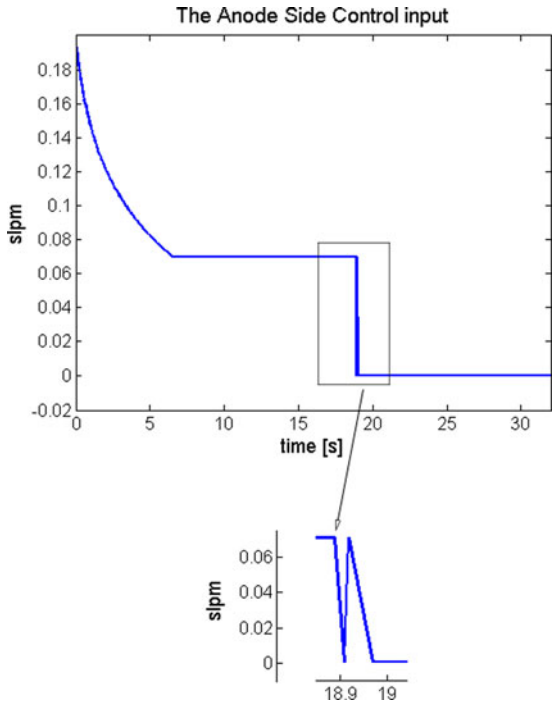

Fig. 6. Control input at the anode side for (14).

It should be emphasized that in the approach of [5], whenever changes of the stack current happen, the waveform looks like the one presented in Fig. 12. For the actual simulation results of [5], see the corresponding Figs. 9 and 10 from that paper. When the sliding mode control technique of this paper is used, no ripples appear as evident from Figs. 3, 4, 8, and 9. The sliding mode controller presented has a good feature to keep hydrogen and oxygen pressures close to each other despite of the abrupt current changes given in Fig. 5. The proposed controller outperforms the feedback linearization-based controller used in [5] for the same PEM fuel cell model.

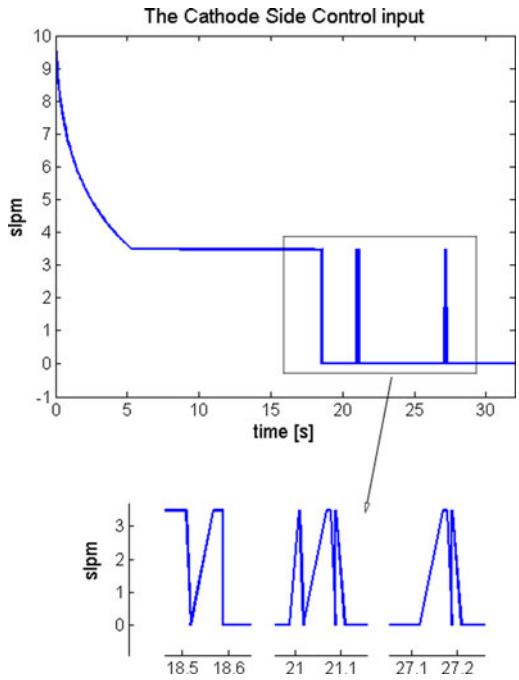

Fig. 7. Control input at the cathode side for (15).

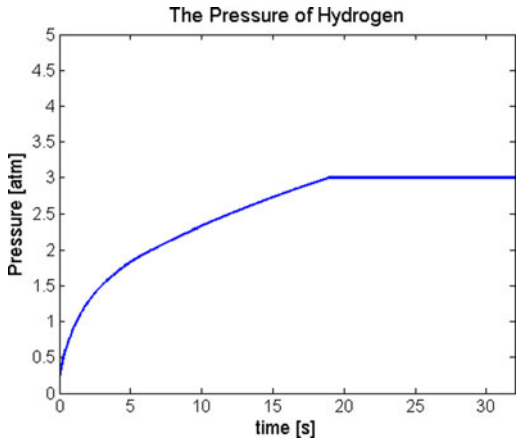

Fig. 8. Pressure of hydrogen for the nonlinear system under the simplified controller (16).

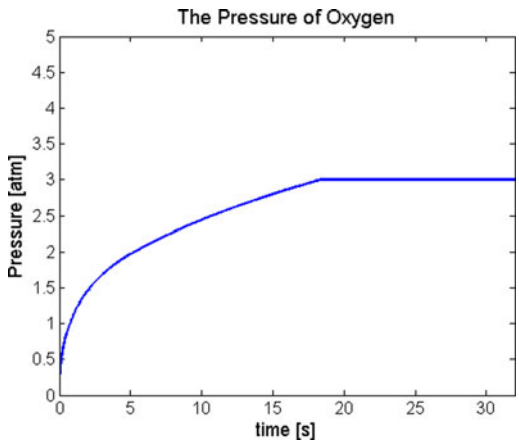

Fig. 9. Pressure of oxygen for the nonlinear system under the simplified controller (17).

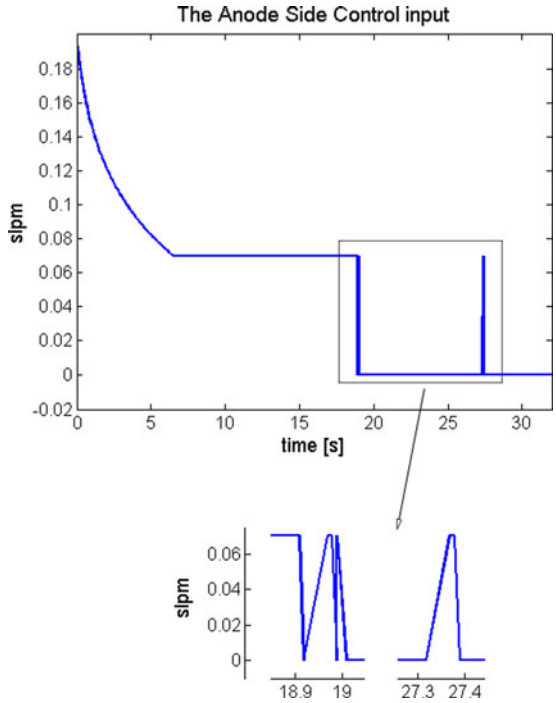

Fig. 10. Control input at the anode side using (16).

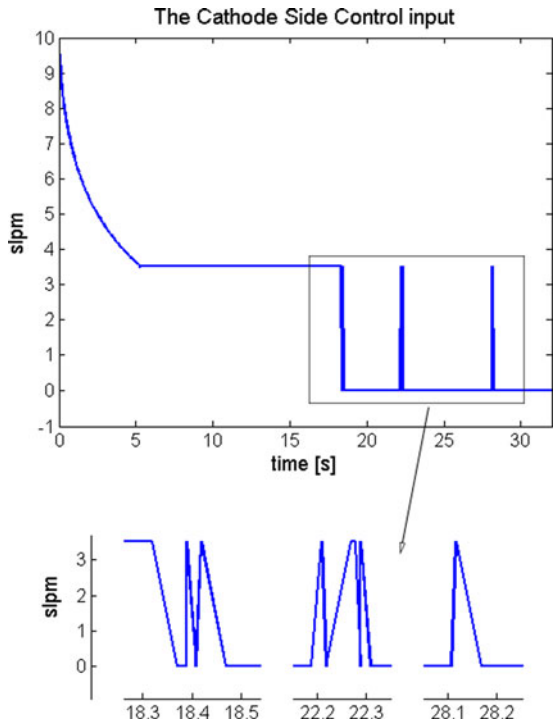

Fig. 11. Control input at the cathode side using (17).

IV. Conclusion and Future Work

We have derived the sliding mode strategy for the well-known nonlinear model of the proton exchange membrane fuel cell. The corresponding simplified sliding mode controller copes very well with the cell current changes, and keeps the pressures of hydrogen and oxygen close to each other and at the desired

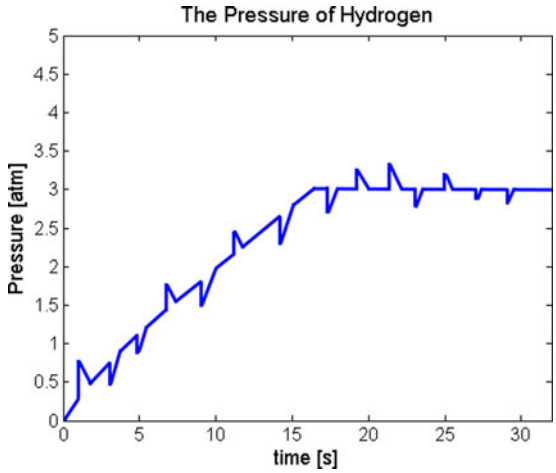

Fig. 12. Example of pressure changes with ripples (using the method of [5]).

values. It outperforms the controller previously used for this model of PEMFC.

In the future, more accurate models of PEMFCs could be and should be developed since "the chemical kinetics in PEMFCs is fast, and the limiting factors in PEMFCs are water and heat transport. And, in the state space modeling in [5], the electrochemical reactions in the catalysts layers and the species transport in the membrane electrolyte assembly are not considered." We believe that our approach with some modifications will be applicable to more complex modes of PEMFCs than the one derived in [5].

REFERENCES

[1] J. Larminie and A. Dicks, *Fuel Cell Systems Explained*. Chichester, U.K.: Wiley, 2000.
[2] M. El-Sharkh, A. Rahman, M. Alam, P. Byrne, A. Sakla, and T. Thomas, "A dynamic model for a stand-alone PEM fuel cell power plant for residential applications," *J. Power Sources*, vol. 138, no. 1–2, pp. 199–204, 2004.
[3] R. S. Gemmen, "Analysis for the effect of inverter ripple current on fuel cell operating condition," *J. Fluids Eng.*, vol. 125, no. 3, pp. 576–585, 2003.
[4] L.-Y. Chiu, B. Diong, and R. Gemmen, "An improved small-signal model of the dynamic behavior of PEM fuel cells," *IEEE Trans. Ind. Appl.*, vol. 40, no. 4, pp. 970–977, Jul./Aug. 2004.
[5] W. Na and B. Gou, "Feedback linearization-based nonlinear control for PEM fuel cells," *IEEE Trans. Energy Convers.*, vol. 23, no. 1, pp. 179–190, Mar. 2008.
[6] J. T. Pukrushpan, A. G. Stefanopoulou, and H. Peng, *Control of Fuel Cell Power Systems*. New York, NY, USA: Springer-Verlag, 2004.
[7] R. Talj, D. Hissel, R. Ortega, and M. Becherif, "Experimental validation of a PEM fuel-cell reduced-order model and a motor-compressor higher order sliding mode control," *IEEE Trans. Ind. Electron.*, vol. 57, no. 6, pp. 1906–1913, Jun. 2010.
[8] C. Kunusch, P. Puleston, M. Mayosky, and J. Riera, "Sliding mode strategy for PEM fuel cells stacks breathing control using a super-twisting algorithm," *IEEE Trans. Control Syst. Technol.*, vol. 17, no. 1, pp. 167–174, Jan. 2009.
[9] I. Matraji, S. Laghrouche, and M. Wack, "Pressure control in a PEM fuel cell via second order sliding mode," *Int. J. Hydrogen Energy*, vol. 37, no. 21, pp. 16 104–16 116, 2012.
[10] W. Garcia-Gabin, F. Dorado, and C. Bordons, "Real-time implementation of a sliding mode controller for air supply on a PEM fuel cell," *J. Process Control*, vol. 20, pp. 325–336, 2010.
[11] G. Wang, Y. Wang, J. Shi, and H. Shao, "Coordinating IMC-PID and adaptive SMC controllers for PEM," *ISA Trans.*, vol. 49, pp. 87–94, 2010.
[12] X. Li, Z.-H. Deng, D. Wei, C.-S. Xu, and G.-Y. Cao, "Novel variable structure control for the temperature of PEM fuel cell stack based on the dynamic thermal affine model," *Energy Convers. Manag.*, vol. 52, no. 11, pp. 3265–3274, 2011.
[13] G. Park and Z. Gajic, "Sliding mode control of a linearized polymer electrolyte membrane fuel cell model," *J. Power Sources*, vol. 212, pp. 226–232, 2012.
[14] A. Hajizadeh and M. Golkar, "Intelligent robust control of hybrid distributed generation system under voltage sag," *Expert Syst. Appl.*, vol. 37, pp. 7627–7638, 2010.
[15] A. Hajizadeh, M. Golkar, and A. Feliachi, "Voltage control and active power management of hybrid fuel-cell/energy-storage power conversion system under unbalanced voltage sag conditions," *IEEE Trans. Energy Convers.*, vol. 25, no. 4, pp. 1195–1208, Dec. 2010.
[16] J.-K. Kuo and C.-F. Wang, "An integrated simulation model for PEM fuel cell power systems with a buck DC-DC converter," *Int. J. Hydrogen Energy*, vol. 36, no. 18, pp. 11 846–11 855, 2011.
[17] F. Zenith and S. Skogestad, "Control of fuel cell power output," *J. Process Control*, vol. 17, no. 4, pp. 333–347, 2007.
[18] B. Gou, W. Na, and B. Diong, *Fuel Cells: Modeling, Control, and Applications*. Boca Raton, FL, USA: CRC Press, 2010.
[19] F. Barbir, *PEM Fuel Cells: Theory and Practice*. New York, NY, USA: Elsevier, 2005.
[20] V. I. Utkin and K. D. Young, "Methods for constructing discontinuity planes in multidimensional variable structure systems," *Autom. Remote Control*, vol. 39, no. 10, pp. 1466–1470, 1978.
[21] W.-C. Su, S. V. Drakunov, and Ü. Özgüner, "Constructing discontinuity surfaces for variable structure systems: A Lyapunov approach," *Automatica*, vol. 32, no. 6, pp. 925–928, 1996.
[22] A. Sinha, *Linear Systems*. Boca Raton, FL, USA: CRC Press, 2007.
[23] B. Drazenovic, "The invariance conditions in variable structure systems," *Automatica*, vol. 5, no. 3, pp. 287–295, 1969.
[24] H. Khalil, *Nonlinear Systems*. Upper Saddle River, NJ, USA: Prentice-Hall, 2002.

Authors' photographs and biographies not available at the time of publication.